CHAPTER 4

The *in vitro* Functional Impairment of Thyroid Hormone Receptor Alpha 1 Isoform Mutants is Mainly Dictated by Reduced Ligand-Sensitivity

Karn Wejaphikul, Anja L.M. van Gucht, Stefan Groeneweg, W. Edward Visser, Theo J. Visser, Robin P. Peeters, Marcel E. Meima

Thyroid *(in press)*

http://hdl.handle.net/1765/119488

4

Abstract

Background: Thyroid hormone (TH) acts on TH receptors (TRs) and regulates gene transcription by binding of TRs to TH response elements (TREs) in target gene promoters. The transcriptional activity of TRs is modulated by interactions with TR-coregulatory proteins. Mutations in TRα cause resistance to thyroid hormone alpha (RTHα). In this study, we analyzed if, beyond reduced T3 affinity, altered interactions with cofactors or different TREs could account for the differential impaired transcriptional activity of different mutants.

Methods: We evaluated four mutants derived from patients (D211G, M256T, A263S, and R384H) and three artificial mutants at equivalent positions in patients with RTHβ (T223A, L287V, and P398H). The *in vitro* transcriptional activity was evaluated on TRE-luciferase reporters (DR4, IR0, and ER6). The affinity for T3 and interaction with coregulatory proteins (NCoR1 and SRC1) were also determined.

Results: We found that the affinity for T3 was significantly reduced for all mutants, except for TRα1-T223A. The reduction in the T3 sensitivity of the transcriptional activity on three TREs, the dissociation of the corepressor NCoR1, and the association of the coactivator SRC1 recruitment for each mutant correlated with the reduced affinity for T3. We did not observe mutation-specific alterations in interactions with cofactors or TREs.

Conclusion: In summary, the degree of impaired transcriptional activity of mutants is mainly determined by their reduced affinity for T3.

Introduction

Genomic actions of thyroid hormone (TH) are regulated by binding of the active form of TH, tri-iodothyronine (T3), to its nuclear TH receptors (TRs), which act predominantly as heterodimers with retinoid X receptors (RXRs) on thyroid hormone response elements (TREs) in the promoter region of target genes (1,2). TREs usually consist of two-consensus half-sites that can be organized in direct repeats (DRs), inverted repeats (IRs), and everted repeats (ERs), separated by a stretch of random nucleotides of various lengths, of which the DR4-TRE is the predominant TR-binding form (3-6). In the absence of ligand, TRs repress target gene transcription by recruitment of corepressors such as nuclear receptor corepressor 1 (NCoR1). Binding of T3 causes dissociation of the corepressors and allows coactivators, such as steroid receptor coactivator 1 (SRC1), to bind to the TR, resulting in activation of gene transcription (1,7).

Mutations in the ligand binding domain (LBD) of TRα1 cause resistance to thyroid hormone alpha (RTHα) which was first described in 2012 (8,9). The phenotype of RTHα patients includes growth retardation, macrocephaly, constipation, intellectual disability, anemia, and a high (F)T3/(F)T4 ratio (10,11). To date, 22 mutations (in a total of 37 patients) have been reported as a cause of RTHα. These mutations can be categorized into two groups based on the type of mutation. The first group consists of truncating mutations caused by nonsense or frameshift mutations that create premature stop codons and shorten the length of the LBD (8,9,12-14). This structural alteration completely abolishes T3 affinity and T3-induced transcriptional activity of TRα1. The second group consists of missense mutations that result in single amino acid substitutions in the LBD (10,13-20). These mutant receptors can still bind T3 but with a lower affinity than wild-type (WT) receptors.

There is a variety in the clinical phenotype of RTHα patients. Patients with truncating mutations generally have a more severe phenotype than patients with missense mutations (9,12-14). Within the latter group, there are notable differences in the neurocognitive features (14,17,20). At present, it is unclear whether these differences are solely explained by differences in T3 binding. In RTHβ, mutation-specific effects on particular TREs and differences in interaction with coactivators versus corepressors have been described (21-24). Here, we studied if mutation-specific effects on TRE or cofactor binding are present in a selected series of seven specific TRα1 missense mutations.

Materials and methods

Plasmid constructs

The coding sequence (cDNA) of full-length TRα1 fused at the 5' end to the FLAG epitope or to VP16 were cloned into the pcDNA3 (9) and the pCMX expression vectors (18),

respectively, as previously described. Selected TRα1 missense mutations were introduced into pcDNA3-FLAG TRα1 and pCMX-VP16 TRα1 expression vectors using the QuickChange II Mutagenesis kit (Align Technologies, Amstelveen, The Netherlands) (see Supplementary Table S1 for primers) and confirmed by Sanger sequencing.

The luciferase reporter constructs containing either direct (DR4), inverted (IR0), or everted repeat (ER6) TRE configurations (TRE-tkLuc) (25), the luciferase reporter construct containing Gal4 binding site (UAStkLuc), and the pSG424 expression vector constructs containing the Gal4 DNA-binding domain (GAL4-DBD) fused to the interacting domains of NCoR1 or SRC1 (8) have all been described elsewhere.

[^{125}I]T3 competitive binding assays

[^{125}I]T3 competitive binding assays were performed as previously described (26). In brief, WT and mutant FLAG-TRα1 proteins were synthesized using the TnT® T7 Quick Coupled Transcription/Translation System (L1170, Promega, Leiden, The Netherlands). The proteins were incubated with 0.02 nM of [^{125}I]T3 (prepared in-house as previously described (27)) and 0-10,000 nM unlabeled T3 (Cat. No. T2877, Sigma-Aldrich) at 30°C for 2 hours. The input of WT and mutant FLAG-TRα1 proteins lysate was adjusted to obtain 10-20% maximal [^{125}I]T3 binding, in order to prevent ligand-depletion effect. TR bound [^{125}I]T3 was measured and calculated as a percentage [^{125}I]T3 input. The dissociation constant (Kd) was computed by GraphPad Prism 5.0 (GraphPad, La Jolla, CA)

In silico model prediction

The various TRα1 mutations were introduced into the WT T3-bound TRα1 crystal structure (PDB-ID: 2H77 (28)) using the side-chain substitution and optimization tools of the YASARA Structure Software (YASARA Bioscience GmbH, Vienna, Austria) (29). The structural models of the TRα1 mutants have been processed and compared to the WT TRα1 structure as previously described (20). Given their location outside the ligand-binding pocket, the D211G, T223A, R384H, and P398H mutant models were compared to WT after additional molecular dynamic simulations in an AMBER force field with water as a solvent to investigate their impact on the structural integrity of the receptor.

Ligand-binding energy was calculated using the BindEnergy command implemented in YASARA Structure Software, which calculates the in *vacuo* binding energy in a NOVA force field without considering solvation effects (30). As such, this approach is suitable for detecting changes in binding energy by mutations that affect substrate interactions directly, and not for those having indirect effects. A high value indicates a favorable T3 binding.

Cell culture and transfection

JEG-3 cells (ECACC Cat# 92120308, RRID:CVCL_0363, Sigma-Aldrich) were cultured in 24-well plates using the growth medium (DMEM/F12 supplemented with 9%FBS,

100 nM Na_2SeO_3, 100 U/mL penicillin, and 100 µg/mL streptomycin) and transfected as previously described (19,26). Briefly, 20 ng of FLAG-TRα1 plasmid was co-transfected with 120 ng TRE-tkLuc reporter construct for transcriptional activity assays. For protein-protein interaction (mammalian two-hybrid) assays, 20 ng of TRα1 fused to the transcriptional activator VP16 (VP16-TRα1) plasmid was co-transfected with 20 ng of NCoR1 or SRC1 fused to the DNA binding domain of Gal4 (GAL4-NCoR1 or GAL4-SRC1) and 120 ng of UAS-tkLuc. In both assays, 20 ng pMaxGFP plasmid was co-transfected to monitor the transfection efficiency. All of the transfection processes were performed in TH-depleted medium (DMEM/F12 supplemented with 9% charcoal-stripped FBS) using Xtreme Gene 9 transfection reagent (Roche Diagnostics, Almere, NL). After 24-hour transfection, cells were stimulated for 24 hours with 0-10,000 nM T3 in DMEM/F12 supplemented with 0.1% bovine serum albumin (BSA).

Immunoblotting

The expression of FLAG- and VP16-TRα1 proteins in cells was verified by immunoblotting nuclear extracts of JEG-3 cells transfected with WT or mutant TR expression constructs as previously described (19,26). The receptors were probed with 1:1000 dilution of FLAG-M2 antibody (#F1804 Sigma-Aldrich) or 1:1000 dilution of VP16 antibody (sc-7545, Santa Cruz Biotechnology). Histone 3 protein was detected with 1:1000 dilution of Histone 3 (H3; 1B1B2) antibody (#14269 Cell Signaling Technology) to verify comparable protein input. Bands were visualized on the Alliance 4.0 Uvitec platform (Uvitec Ltd) by Enhanced Chemiluminescence (Thermofisher Scientific).

Electrophoretic mobility shift assays (EMSA)

A double-stranded overlapping oligonucleotide probe containing DR4-TRE was obtained by annealing 25 ng of sense and antisense oligonucleotides 5'end labeling with fluorescence dye (5'IRDye®700) (Integrated DNA Technologies, Leuven, Belgium) at 80°C for 5 minutes (sense oligonucleotides: 5'-AGGACGTTGGGGTTAGGGGAGGACAGTGGAC-3', antisense oligonucleotides: 5'-GTCCACTGTCCTCCCCTAACCCCAACGTCCT-3'). The DR4-TRE probe was diluted to a final concentration of 1 ng/µL in 50 µL 1xTE buffer (10mM Tris HCl pH 8.0, 1 mM EDTA). FLAG-TRα1 and RXRα proteins were synthesized by the TnT® T7 Quick Coupled Transcription/Translation System (L1170, Promega, Leiden, The Netherlands). Since equal amounts of *in vitro* translated receptors were detected on an immunoblot (data not shown), we decided to use 1 µL of *in vitro* translated WT or mutant FLAG-TRα1 and 2 µL of *in vitro* translated RXRα. TR and RXRα were co-incubated in the dark with 0.5 µL of DR4-TRE probe, and 2 µg of poly(deoxyinosinic-deoxycytidylic) acid sodium salt (SC-286691, Santa Cruz Biotechnology) in a final 10 µL of binding buffer (10x binding buffer: 100mM Tris, 10 mM EDTA, 1M KCl, 1 mM DDT, 50% glycerol, 0.1 mg/mL BSA) for 30 minutes at room temperature. Gel electrophoresis was performed on 6%DNA retardation gel (EC6365BOX, Invitrogen). The TR-DNA complexes and residual unbound probe were visualized using an Odyssey® imaging system (LI-COR, Leusden, The Netherlands).

Luciferase assays

Luciferase activity was determined using the Dual Glo Luciferase kit (E2940, Promega, Leiden, The Netherlands). Luciferase and GFP activities were measured by a luminometer (Victor™ X4, PerkinElmer, Groningen, The Netherlands). Half-maximal effective T3 concentration (EC_{50}), half-maximal inhibitory T3 concentration (IC_{50}), and %WT maximal response were analyzed using GraphPad Prism 5.0 (GraphPad, La Jolla, CA)

Statistical analysis

The statistical differences between WT and mutants were analyzed by One sample T-tests. The statistical differences of fold changes of logKd, logEC_{50}, and logIC_{50} between WT and mutants were determined by one-way ANOVA with Tukey's post-test. Statistical significance was considered at p-values < 0.05.

Results

Selection of mutants

We tested seven TRα1 mutants, of which four were derived from RTHα patients (D211G (19), M256T (20), A263S, and R384H (14)). These mutations covered the three CpG-rich regions of the LBD of TRα1 that are equivalent to the mutation-prone hotspots of the TRβ1 receptor, namely R384H in cluster 1, M256T and A263S in cluster 2, and D211G in cluster 3. The other three mutations were derived from RTHβ patients. TRα1-P398H (cluster 1), the equivalent of TRβ1-P452H, gave rise to an unusual phenotype that included obesity and marked metabolic disturbances in a murine model for RTHα (31). TRα1-T223A (cluster 3) is the equivalent of TRβ1-T277A, which was previously shown to specifically impair transcriptional activity on an ER6-TRE and diminish affinity for SRC-1 (24). Finally, TRα1-L287V (cluster 2) is the equivalent of TRβ1-L341V, a recently identified mutation that causes a strong decrease in T3-binding affinity and a concomitant reduction in the T3-sensitivity of transcriptional activity and cofactor recruitment (26).

T3 binding affinity of the TRα1 mutants

We first determined the binding affinity of *in vitro* translated mutant receptors using a [^{125}I]T3 competitive binding assay. The [^{125}I]T3 binding curves were shifted to the right for most mutants (Figure 1A), which reflects a higher required dose of T3 to saturate binding and hence a lower binding affinity. The dissociation constant (Kd) which is the concentration of T3 at which half the binding sites are occupied, varied between mutants (Figure 1B and Supplementary Table S2). TRα1-M256T showed the lowest affinity, as is illustrated by the highest Kd of all mutants (160-fold higher than WT). Binding of T3 was similarly affected for

TRα1-D211G (Kd 25-fold higher than WT), -R384H (25-fold), -L287V (19-fold), and -P398H (17-fold), but significantly less impaired for TRα1-A263S (Kd 5-fold higher than WT) whereas the Kd of TRα1-T223A was not different from WT. These data indicate that the binding affinity is reduced to a different extent for the different mutants.

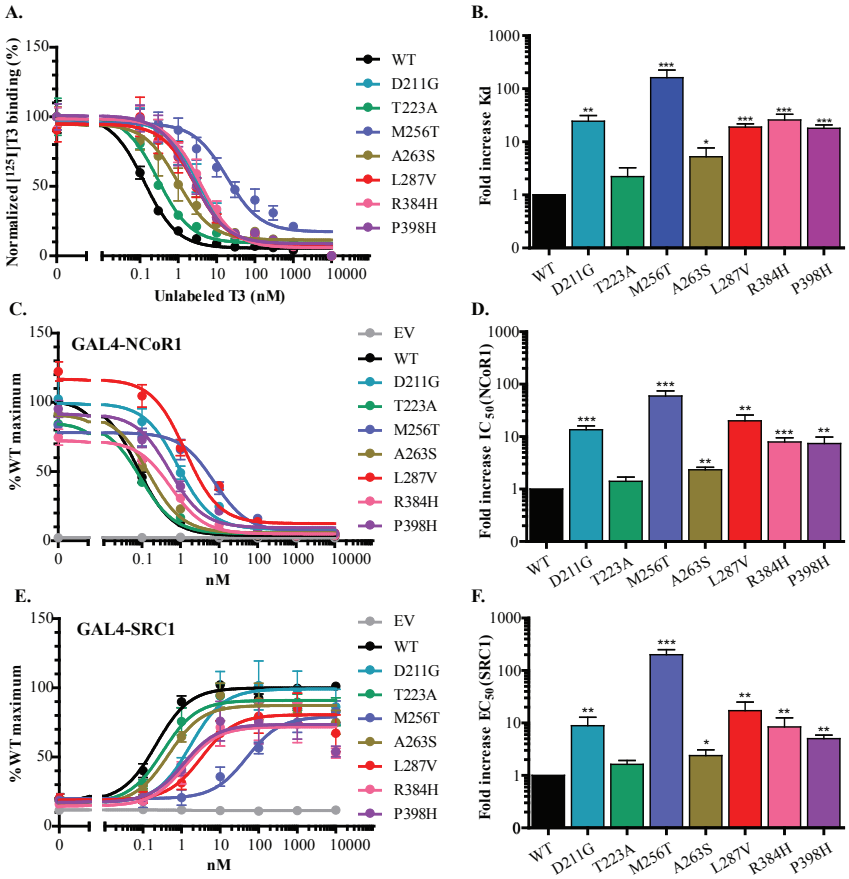

Figure 1. (A-B) [^{125}I]T3 competitive binding assays of the TRα1 WT and mutants. (A) The dissociation curves of all mutants are shifted to the right, indicative of a reduced T3 binding affinity. (B) The fold increase of the Kd are various between mutants (One-sample T-test, *P<0.05, **P<0.01, ***P<0.001). Data presented as mean ± SEM from four independent experiments performed in duplicate. (C-F) Mammalian two-hybrid assays demonstrating TRα1-cofactor interactions. (C) T3-induced GAL4-NCoR1 dissociation and (E) GAL4-SRC1 association curves show a various degree of reduced T3-dependent NCoR1 release and SRC1 recruitment of mutants, respectively. These are indicated by the right shift of the curves and higher IC_{50}-NCoR1 or EC_{50}-SRC1 than that of WT. (D) The fold increases in IC_{50} for the NCoR1 dissociation are similar to (E) the fold increase in EC_{50} for the SRC1 association for each mutation (the fold increases IC_{50}-NCoR1 and EC_{50}-SRC1 of the mutants were compared to WT by One-sample T-test; *P<0.05, **P<0.01, ***P<0.001). Data presented as mean ± SEM from at least four independent experiments performed in triplicate.

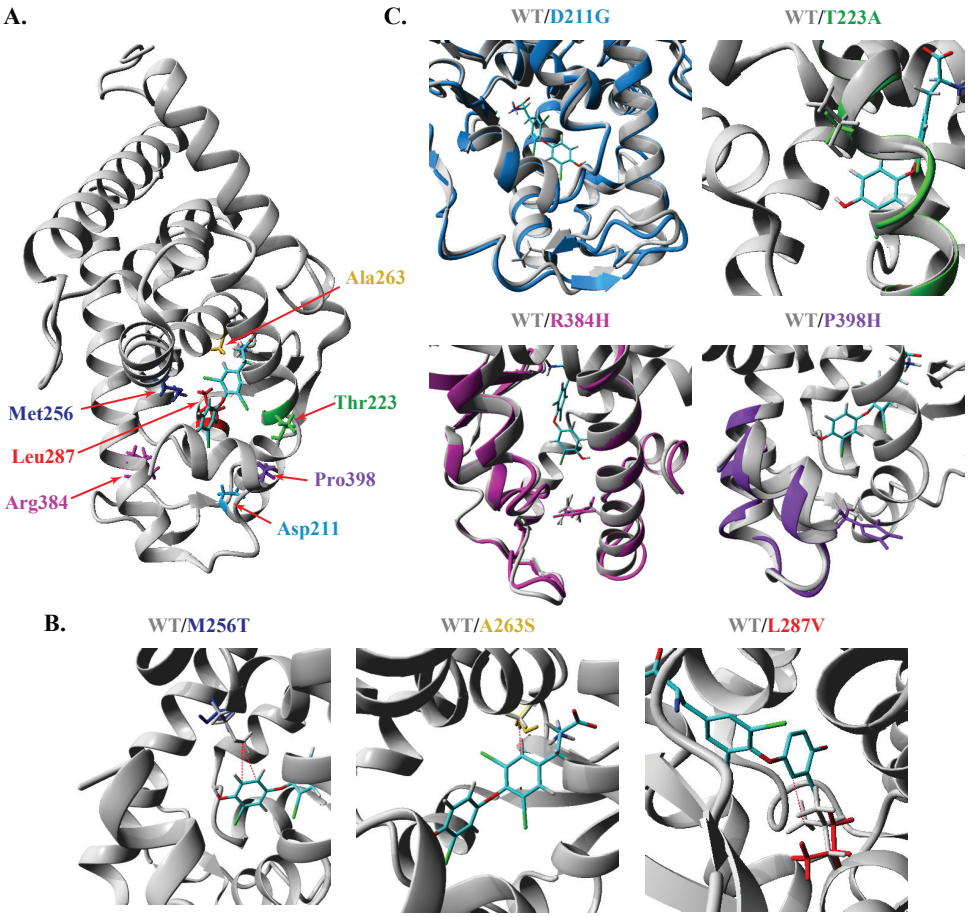

Figure 2. (A) The WT TRα1 crystal structure in complex with T3 (PDB ID: 2H77) in which the locations of the mutated residues studied are highlighted. (B) Close-up view of the TRα1 ligand-binding pocket, presented as an overlay of the WT crystal (grey) and indicated mutant models (colored). The side-chains of the mutant residues are displayed in blue (M256T, left panel), orange (A263S, middle panel), and red (L287V, right panel) and of the corresponding WT residues in grey. Hydrophobic interactions between WT residues and T3 are indicated with a red dashed line. The interaction between mutant residues and T3 are not observed. For clarity, the small deviations in the carbon-backbone structure are not displayed. (C) Close-up view of the overlay of the WT TRα1 structure and models with indicated mutations that affect residues outside the ligand-binding pocket. Mutant models are displayed in blue (D211G, left upper panel), green (T223A, right upper panel), pink (R384H, left lower panel), and purple (P398H, right lower panel), and WT TRα1 in grey. The T3 ligand is displayed in all panels in element color. All figures were created in YASARA Structure using PovRay imaging software.

In silico model of mutant TRα1

Structural modeling was used to validate our *in vitro* studies. The side-chains of Ala263, Met256, and Leu287 face to the ligand-binding pocket (Figure 2A and 2B) and are predicted to make direct interactions with T3 (Supplementary Figure S1). The hydrophobic interaction between the side-chain of Ala263 and the inner ring of T3 is lost in the A263S mutant. As previously reported (20), the M256T abrogates the direct interactions of Met256 with T3 and simultaneously disturbs the structural niche accommodating the outer ring of T3. In analogy to the predicted *in silico* effects of the L341V mutant in TRβ1 (26), the L287V mutant disrupts the direct hydrophobic interaction of Leu287 with T3. In agreement with our *in vitro* studies, all three mutations reduced the calculated T3-binding energy compared to WT TRα1 in the order M256T>L287V>A263S (Supplementary Figure 1D). Due to their location outside the binding pocket, the side-chains of Asp211, Arg384, Pro398 (facing other internal domains), and Thr223 (facing the external protein surface), do not make direct contact with T3 (Figure 2A and 2C), which prevents reliable *in silico* prediction of their impact on binding affinity. Structural modeling revealed extensive structural changes for the D211G (predominantly within the loop connecting H2 and H3), R384H and P398H (predominantly H11 and H12) mutants, whereas the T223A mutant displayed only minor local structural changes of the backbone configuration (Figure 2C). These observations may well explain the differential effects of these mutations on *in vitro* binding affinity.

Heterodimerization of TRα1 mutants with RXRα

To determine whether the dimerization of the mutants with RXR and binding of the dimer to DNA was affected, we performed electrophoretic mobility shift assays (EMSAs) with *in vitro* translated WT or mutant TRα1 and RXRα on a fluorescently labeled DR4-TRE (Supplementary Figure S2). The result showed that only a co-incubation of TRα1 and RXRα could shift the DR4-TRE oligonucleotide probe upward. The upward shift of the probe was not observed in an incubation of WT TRα1 or RXRα alone. These findings indicate that the WT receptors exclusively bound to the DR4-TRE as heterodimers with RXRα, which is in contrast to the TRβ1 isoform that can bind as both homo- and heterodimers (32,33). The intensity of the heterodimer band was similar to WT for all mutants. In addition, heterodimer binding to the DR4-TRE was independent of the presence of T3 for WT and mutants. These results show that heterodimerization with RXRα and binding to the DR4-TRE is not affected in any of the mutants.

Receptor-cofactor interaction of the TRα1 mutants

To determine whether cofactor recruitment of the mutants was impaired, we next evaluated the interaction of the mutants with the corepressor NCoR1 and the coactivator SRC1, which directly bind to TRs and play a crucial role in receptor function (1,7). In a mammalian two-hybrid assay, VP16-TRα1 activates a luciferase reporter (UAS-tkLuc) only when it interacts with GAL4-NCoR1 or -SRC1. As a measure for T3-dependence, we

determined the concentration that gave half-maximum dissociation of NCoR1 (IC_{50}) and half-maximum association of SRC1 (EC_{50}). Stimulation of WT TRα1 with low concentrations of T3 (0.1-1 nM) already resulted in dissociation of GAL4-NCoR1 (IC_{50} 0.08 nM) and association of GAL4-SRC1 (EC_{50} 0.28 nM). Most mutants required higher T3 concentrations to dissociate from NCoR1 (Figure 1C) and recruit SRC1 (Figure 1E). Consistent with the affinity for T3, TRα1-M256T showed the highest IC_{50} for NCoR1 dissociation (60-fold higher than WT) and EC_{50} for SRC1 association (200-fold) (Figure 1D, 1F, Supplementary Figure S3, and Supplementary Table S3). The TRα1-D211G, L287V, R384H, and P398H mutants showed higher IC_{50}-NCoR1 dissociation and EC_{50}-SRC1 association than WT but lower than TRα1-M256T. The fold increase IC_{50} and EC_{50} of these four mutations were similar. The IC_{50}-NCoR1 dissociation and EC_{50}-SRC1 association of A263S-TRα1 mutation were approximately two-fold higher than WT, corresponding to the changes of its Kd in competitive binding assays. For TRα1-T223A, the T3-induced NCoR1 dissociation and SRC1 association were similar to the WT receptor. We did not observe major differences in maximal binding of either NCoR1 or SRC1 to mutants compared to WT, indicating that the affinity of the mutants for these cofactors is not markedly disturbed.

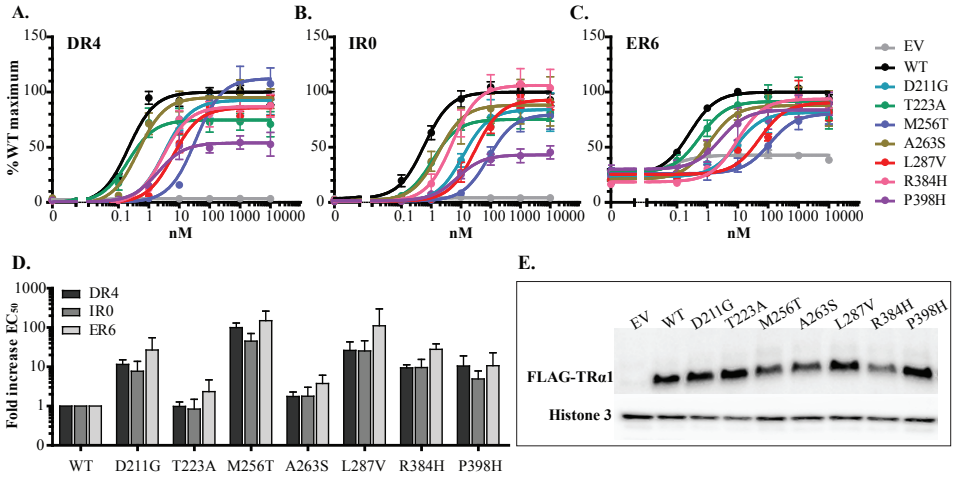

Figure 3. The T3-induced transcriptional activity of TRα1 WT and mutants tested on three different TRE-luciferase reporter constructs. (A-C) The dose-response curves show a various degree of impaired transcriptional activity of mutants, as indicated by the right shift of the curves and higher EC_{50} than WT. (D) The fold increases of mutants' EC_{50} are various between mutations. The shift of EC_{50} on three TREs generally follows a similar trend for each mutation. Data presented as mean ± SEM from at least three independent experiments performed in triplicate. (E) Immunoblot confirms the expression of WT and mutant FLAG-TRα1 in JEG-3 cells.

Transcriptional activity of the TRα1 mutants

We then tested the mutants for transcriptional activity using a reporter assay. For this, we co-transfected WT or mutant receptors into JEG-3 cells with constructs in which the coding sequence for firefly luciferase is under control of a DR4, IR0 or ER6-TRE.

The T3-induced transcriptional activity on the DR4-TRE was impaired for most mutant receptors, as indicated by a rightward shift of the dose-response curves as compared to WT and a concomitant increase in EC_{50}, representing the T3 dose that is needed to achieve a half-maximal response. (Figure 3A and Supplementary Table S4). TRα1-M256T had the highest EC_{50} (100-fold higher than WT). The EC_{50} of TRα1-D211G, L287V, R384H, and P398H was approximately 10 to 20-fold higher than that of WT. In contrast, the EC_{50} of TRα1-A263S and T223A was not significantly different from WT. The fold increase in EC_{50} tested on the IR0- and ER6-TREs of each mutant was not significantly different from that tested on the DR4-TRE (Figure 3B-D), suggesting that the effects of these mutations are not TRE-specific. Most of the mutants showed a similar maximal transcriptional activity as WT at supraphysiological T3 concentrations, with the exception of TRα1-T223A on DR4-TRE and TRα1-P398H on DR4- and IR0-TRE that were significantly lower than that of WT.

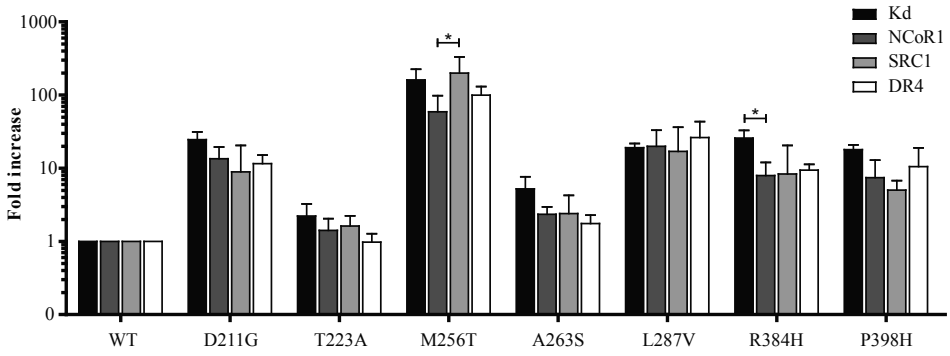

Figure 4. Fold increases of Kd, IC_{50}-NCoR1 dissociation, EC_{50}-SRC1 association and EC_{50} of T3-induced transcriptional activity on the DR4-TRE. These fold increases are various among mutants but generally follow a similar trend for each mutant, except for M256T and R384H (One-way ANOVA with Tukey's post-test *P<0.05).

Correlation between T3-affinity, cofactor binding, and transcriptional activity of TRα1 mutants

Finally, in order to determine whether certain aspects of receptor regulation were proportionally stronger affected than that would be expected from the effect of the mutation on T3-binding, we correlated the fold increase of parameters for binding affinity, and T3-dependent activity and cofactor recruitment (Figure 4). The fold increases in IC_{50}-NCoR1,

EC_{50}-SRC1, and EC_{50} on DR4-TRE generally followed the same trend as the fold increase in Kd of each mutant with two exceptions. First, the fold increase in EC_{50}-SRC1 of TRα1-M256T was slightly but significantly higher than its IC_{50}-NCoR1, which would suggest a marginally stronger effect of the mutation on T3-dependent SRC1 recruitment than NCoR1 release. Second, the fold increase in Kd of TRα1-R384H was slightly higher than its IC_{50}-NCoR1. In both cases, however, this did not result in a significant effect on the EC_{50}-DR4 TRE, indicating that these differences do not majorly contribute to the degree of functional impairment.

Discussion

In the current study, we report *in vitro* functional studies of seven TRα1 missense mutations. The main purpose was to investigate if other factors, beyond disturbed T3 binding, contribute to the functional impairment of TRα1 mutations. According to our results, the reduced affinity for T3 is the main factor that determines both the severity of impaired transcriptional activity as well as impaired TR-cofactor interaction of the mutants. In our series, we did not find evidence for mutation-specific effects on different TREs or coregulatory protein binding.

Our selection of mutants covered the equivalents of the three mutation-prone hotspots in TRβ1. We evaluated the effect of the mutations on the transcriptional activity by overexpressing WT or mutant receptors with a reporter gene under control of TREs. Since some TRβ1 mutants display TRE selective defects, we included all three reported half-site configurations (DR4, IR0, and ER6). As expected, the mutants had an impaired T3-dependent transcriptional activity, as illustrated by their dose-response curves with a clear shift to the right side of the WT curve and corresponding higher EC_{50} than WT. The degree of impaired transcriptional activity varied among the mutants and correlated with the reduced T3-binding energy of the mutants predicted by the *in silico* modeling and the reduction in T3-affinity from the *in vitro* binding assays. This finding is in line with previous reports of the other mutants derived from RTHα patients (8,12,15,25). In addition, the degree of impaired transcriptional activity seemed to be related to the severity of the phenotype of the RTHα patients, especially the delayed motor development which is much more prominent in the patients carrying TRα1-D211G and -R384H mutations than in the patient carrying a TRα1-A263S mutation. This is in agreement with a previous report by Moran et al. that showed that the functional properties of two TRα1 mutations (A263V and L274P) correlate with the clinical features of the patients (18).

There was no TRE-selective reduction in T3-dependent receptor activity since the fold increase in EC_{50} on all three TREs was similar for each mutant. Of note, the T223A-TRα1 mutant did not show any differential effect on different TREs, which is in contrast with its equivalent TRβ1-T277A, which is selectively affected on an ER6-TRE (24). However, the maximal response of T223A and P398H were lower than that of WT on the DR4- and

IR0-TRE. This TRE-specific submaximal response has been previously reported in TRβ1-T277A (24); however, in these studies the submaximal response was found on the DR4- and ER6-TRE. The TRE-specific transcriptional impairment may be caused by different patterns of dimer formation and cofactor recruitment among TREs (34,35). Nevertheless, since numerous chromatin occupation studies have suggested that the DR4-TRE is the most important TRE playing a role in the *in vivo* TR transcription (3-6), the pattern of TR-regulating gene transcription is more likely to follow the *in vitro* result of DR4-TRE rather than IR0- and ER6-TRE. Therefore, selective transcriptional impairment of the mutants on IR0- and ER6-TRE found *in vitro* may not have a large contribution in the severity of phenotypes in RTH patients.

It has been shown that submaximal response of mutant receptors can be caused by impaired TR-cofactor interactions. For instance, the reduced maximal response of TRβ1-T277A was due to a reduced affinity for SRC1, which could be rescued by overexpression of SRC1 (24). Mutations at the residues adjacent to the Pro452 of the TRβ1 (homologous to Pro398 of TRα1), Pro453 and Leu454, were also unable to reach WT maximal response and have been shown to have a defective TR-cofactor interaction that consequently affects transcriptional activity to a greater extent than what would be expected based on their reduced affinity for T3 (25,36,37). We, therefore, evaluated the interaction of selected TRα1 mutants with the NCoR1 corepressor and the SRC1 coactivator. Except for T223A, the mutants required higher T3 levels than WT to dissociate from NCoR1 and to associate with SRC1, illustrating the impaired T3-dependent TR-cofactor interaction of these mutants. However, the degree of impaired TR-cofactor interaction was similar to the reduced affinity for T3 for all selected mutants. In addition, the maximum binding of TRα1-T223A and -P398H was similar to WT. These findings suggest that these mutations alter the T3-dependent TRα1-cofactor recruitment via their reduced T3 affinity, but that the submaximal response is likely explained by another mechanism such as impaired interaction of the mutants with other nuclear cofactors. For this reason, we also studied the heterodimerization property of the selected TRα1 mutants and found that none of them disturbed heterodimer formation on the DR4-TRE, suggesting that the submaximal response of these mutant receptors is not explained by altered heterodimerization with RXR.

To our knowledge, our study reports the *in vitro* functional impairment at different levels of the largest series of TRα1 mutants to date, including four mutations derived from RTHα patients which cover all three CpG-rich clusters of TRα1 that correspond with the mutation-prone hotspots of TRβ1. However, the transcriptional activation of mutants in this study was only tested on the most abundant TRE configuration, DR4 (3-6), and the other two well-known TRE configurations, IR0 and ER6, which do not cover all natural TREs. Therefore, the results should be interpreted and applied cautiously. Our study also did not explore some issues that might complicate the phenotype of RTH patients, for instance, the negative transcriptional gene regulation by TRs and the effect of mutant TRs on WT receptor function, as known as a dominant-negative effect. In addition, our experiments were performed exclusively *in*

vitro and mainly by the overexpressing system in the JEG-3 cells which might not be entirely comparable to the *in vivo* situation. Although JEG-3 cells comprise a well-established model to study the impact of TRs mutations, the results of which correlating with the severity of the clinical phenotype, it may not represent the situation in other cell types or tissues. Therefore, studies in different TR-overexpressing cell lines, or in models that rely on endogenously expressed mutant TRs (such as CRISPR-Cas9 genome editing or primary cells derived from patients) may substantiate our findings.

RTHα patients are currently treated with levothyroxine (LT4) to normalize FT4 levels and reduce the hypothyroid state of tissues that predominantly express TRα1, which in some cases has been shown to ameliorate the developmental delay and chronic symptoms (15,18,19), however, the working mechanism is yet unclear. Since FT4 and T3 levels are only marginally increased, it seems unlikely that this treatment results in a significant occupation of receptors that have 10 to 100-fold reduction in ligand affinity, but rather increases the number of activated WT receptors. Given that the functional defects of TRα1 missense mutants are driven by their reduced ligand-affinity, agonists that provide a better fit to the altered ligand-binding pockets could, therefore, be a tailor-made treatment. Although such agonists are currently lacking, the finding that some TRβ1 mutants are more efficiently dissociated from NCoR1 by the natural T3 analogue triiodoacetic acid (TRIAC), which is sometimes used to suppress FT4 levels in RTHβ patients, and the TR antagonist NH-3 (38), shows that such an approach may be viable.

In summary, this study demonstrates that the severity of impaired transcriptional activity of mutant TRα1 receptors is mainly determined by the reduced affinity for T3. These mutations also alter TR-cofactor interactions to the same magnitude as the T3 binding defect. However, further studies are required to extensively evaluate the *in vivo* consequences of the TRα1 mutations.

Acknowledgements

We would like to thank Prof. V. Krishna Chatterjee (Wellcome-MRC Institute of Metabolic Science, University of Cambridge, United Kingdom) for kindly providing some of the plasmids used in this study. This work is supported by Zon-MWTOP Grant 91212044 and an Erasmus MC Medical Research Advisory Committee (MRACE) grant (RPP, MEM), and Chiang Mai University (KW).

Author Disclosure Statement

The authors have nothing to disclose.

References

1. Cheng SY, Leonard JL, Davis PJ. Molecular aspects of thyroid hormone actions. *Endocr Rev.* 2010;**31**(2):139-170.
2. Flamant F, Cheng SY, Hollenberg AN, Moeller LC, Samarut J, Wondisford FE, Yen PM, Refetoff S. Thyroid Hormone Signaling Pathways: Time for a More Precise Nomenclature. *Endocrinology.* 2017;**158**(7):2052-2057.
3. Chatonnet F, Guyot R, Benoit G, Flamant F. Genome-wide analysis of thyroid hormone receptors shared and specific functions in neural cells. *Proc Natl Acad Sci U S A.* 2013;**110**(8):E766-775.
4. Ayers S, Switnicki MP, Angajala A, Lammel J, Arumanayagam AS, Webb P. Genome-wide binding patterns of thyroid hormone receptor beta. *PLoS One.* 2014;**9**(2):e81186.
5. Grontved L, Waterfall JJ, Kim DW, Baek S, Sung MH, Zhao L, Park JW, Nielsen R, Walker RL, Zhu YJ, Meltzer PS, Hager GL, Cheng SY. Transcriptional activation by the thyroid hormone receptor through ligand-dependent receptor recruitment and chromatin remodelling. *Nat Commun.* 2015;**6**:7048.
6. Ramadoss P, Abraham BJ, Tsai L, Zhou Y, Costa-e-Sousa RH, Ye F, Bilban M, Zhao K, Hollenberg AN. Novel mechanism of positive versus negative regulation by thyroid hormone receptor beta1 (TRbeta1) identified by genome-wide profiling of binding sites in mouse liver. *J Biol Chem.* 2014;**289**(3):1313-1328.
7. Astapova I. Role of co-regulators in metabolic and transcriptional actions of thyroid hormone. *J Mol Endocrinol.* 2016;**56**(3):73-97.
8. Bochukova E, Schoenmakers N, Agostini M, Schoenmakers E, Rajanayagam O, Keogh JM, Henning E, Reinemund J, Gevers E, Sarri M, Downes K, Offiah A, Albanese A, Halsall D, Schwabe JW, Bain M, Lindley K, Muntoni F, Vargha-Khadem F, Dattani M, Farooqi IS, Gurnell M, Chatterjee K. A mutation in the thyroid hormone receptor alpha gene. *N Engl J Med.* 2012;**366**(3):243-249.
9. van Mullem A, van Heerebeek R, Chrysis D, Visser E, Medici M, Andrikoula M, Tsatsoulis A, Peeters R, Visser TJ. Clinical phenotype and mutant TRalpha1. *N Engl J Med.* 2012;**366**(15):1451-1453.
10. van Gucht ALM, Moran C, Meima ME, Visser WE, Chatterjee K, Visser TJ, Peeters RP. Resistance to Thyroid Hormone due to Heterozygous Mutations in Thyroid Hormone Receptor Alpha. *Curr Top Dev Biol.* 2017;**125**:337-355.
11. Moran C, Chatterjee K. Resistance to Thyroid Hormone alpha-Emerging Definition of a Disorder of Thyroid Hormone Action. *J Clin Endocrinol Metab.* 2016;**101**(7):2636-2639.
12. Moran C, Schoenmakers N, Agostini M, Schoenmakers E, Offiah A, Kydd A, Kahaly G, Mohr-Kahaly S, Rajanayagam O, Lyons G, Wareham N, Halsall D, Dattani M, Hughes S, Gurnell M, Park SM, Chatterjee K. An adult female with resistance to thyroid hormone mediated by defective thyroid hormone receptor alpha. *J Clin Endocrinol Metab.* 2013;**98**(11):4254-4261.
13. Tylki-Szymanska A, Acuna-Hidalgo R, Krajewska-Walasek M, Lecka-Ambroziak A, Steehouwer M, Gilissen C, Brunner HG, Jurecka A, Rozdzynska-Swiatkowska A, Hoischen A, Chrzanowska KH. Thyroid hormone resistance syndrome due to mutations in the thyroid hormone receptor alpha gene (THRA). *J Med Genet.* 2015;**52**(5):312-316.
14. Demir K, van Gucht AL, Buyukinan M, Catli G, Ayhan Y, Bas VN, Dundar B, Ozkan B, Meima ME, Visser WE, Peeters RP, Visser TJ. Diverse Genotypes and Phenotypes of Three Novel Thyroid Hormone Receptor-alpha Mutations. *J Clin Endocrinol Metab.* 2016;**101**(8):2945-2954.
15. Moran C, Agostini M, Visser WE, Schoenmakers E, Schoenmakers N, Offiah AC, Poole K, Rajanayagam O, Lyons G, Halsall D, Gurnell M, Chrysis D, Efthymiadou A, Buchanan C, Aylwin S, Chatterjee KK. Resistance to thyroid hormone caused by a mutation in thyroid hormone receptor (TR)alpha1 and TRalpha2: clinical, biochemical, and genetic analyses of three related patients. *Lancet Diabetes Endocrinol.* 2014;**2**(8):619-626.
16. Espiard S, Savagner F, Flamant F, Vlaeminck-Guillem V, Guyot R, Munier M, d'Herbomez M, Bourguet W, Pinto G, Rose C, Rodien P, Wemeau JL. A Novel Mutation in THRA Gene

Associated With an Atypical Phenotype of Resistance to Thyroid Hormone. *J Clin Endocrinol Metab.* 2015;**100**(8):2841-2848.

17. Kalikiri MK, Mamidala MP, Rao AN, Rajesh V. Analysis and functional characterization of sequence variations in ligand binding domain of thyroid hormone receptors in autism spectrum disorder (ASD) patients. *Autism Res.* 2017;**10**(12):1919-1928.
18. Moran C, Agostini M, McGowan A, Schoenmakers E, Fairall L, Lyons G, Rajanayagam O, Watson L, Offiah A, Barton J, Price S, Schwabe J, Chatterjee K. Contrasting Phenotypes in Resistance to Thyroid Hormone Alpha Correlate with Divergent Properties of Thyroid Hormone Receptor alpha1 Mutant Proteins. *Thyroid.* 2017;**27**(7):973-982.
19. van Gucht AL, Meima ME, Zwaveling-Soonawala N, Visser WE, Fliers E, Wennink JM, Henny C, Visser TJ, Peeters RP, van Trotsenburg AS. Resistance to Thyroid Hormone Alpha in an 18-Month-Old Girl: Clinical, Therapeutic, and Molecular Characteristics. *Thyroid.* 2016;**26**(3):338-346.
20. Wejaphikul K, Groeneweg S, Hilhorst-Hofstee Y, Chatterjee VK, Peeters RP, Meima ME, Visser WE. Insight into molecular determinants of T3 vs. T4 recognition from mutations in thyroid hormone receptor alpha and beta. *J Clin Endocrinol Metab.* 2019;**104**(8):3491-3500.
21. Clifton-Bligh RJ, de Zegher F, Wagner RL, Collingwood TN, Francois I, Van Helvoirt M, Fletterick RJ, Chatterjee VK. A novel TR beta mutation (R383H) in resistance to thyroid hormone syndrome predominantly impairs corepressor release and negative transcriptional regulation. *Mol Endocrinol.* 1998;**12**(5):609-621.
22. Safer JD, Cohen RN, Hollenberg AN, Wondisford FE. Defective release of corepressor by hinge mutants of the thyroid hormone receptor found in patients with resistance to thyroid hormone. *J Biol Chem.* 1998;**273**(46):30175-30182.
23. Huber BR, Desclozeaux M, West BL, Cunha-Lima ST, Nguyen HT, Baxter JD, Ingraham HA, Fletterick RJ. Thyroid hormone receptor-beta mutations conferring hormone resistance and reduced corepressor release exhibit decreased stability in the N-terminal ligand-binding domain. *Mol Endocrinol.* 2003;**17**(1):107-116.
24. Collingwood TN, Wagner R, Matthews CH, Clifton-Bligh RJ, Gurnell M, Rajanayagam O, Agostini M, Fletterick RJ, Beck-Peccoz P, Reinhardt W, Binder G, Ranke MB, Hermus A, Hesch RD, Lazarus J, Newrick P, Parfitt V, Raggatt P, de Zegher F, Chatterjee VK. A role for helix 3 of the TRbeta ligand-binding domain in coactivator recruitment identified by characterization of a third cluster of mutations in resistance to thyroid hormone. *EMBO J.* 1998;**17**(16):4760-4770.
25. Collingwood TN, Adams M, Tone Y, Chatterjee VK. Spectrum of transcriptional, dimerization, and dominant negative properties of twenty different mutant thyroid hormone beta-receptors in thyroid hormone resistance syndrome. *Mol Endocrinol.* 1994;**8**(9):1262-1277.
26. Wejaphikul K, Groeneweg S, Dejkhamron P, Unachak K, Visser WE, Chatterjee VK, Visser TJ, Meima ME, Peeters RP. Role of Leucine 341 in Thyroid Hormone Receptor Beta Revealed by a Novel Mutation Causing Thyroid Hormone Resistance. *Thyroid.* 2018;**28**(12):1723-1726.
27. Mol JA, Visser TJ. Synthesis and some properties of sulfate esters and sulfamates of iodothyronines. *Endocrinology.* 1985;**117**(1):1-7.
28. Nascimento AS, Dias SM, Nunes FM, Aparicio R, Ambrosio AL, Bleicher L, Figueira AC, Santos MA, de Oliveira Neto M, Fischer H, Togashi M, Craievich AF, Garratt RC, Baxter JD, Webb P, Polikarpov I. Structural rearrangements in the thyroid hormone receptor hinge domain and their putative role in the receptor function. *J Mol Biol.* 2006;**360**(3):586-598.
29. Krieger E, Vriend G. YASARA View - molecular graphics for all devices - from smartphones to workstations. *Bioinformatics.* 2014;**30**(20):2981-2982.
30. Krieger E, Koraimann G, Vriend G. Increasing the precision of comparative models with YASARA NOVA--a self-parameterizing force field. *Proteins.* 2002;**47**(3):393-402.
31. Liu YY, Schultz JJ, Brent GA. A thyroid hormone receptor alpha gene mutation (P398H) is associated with visceral adiposity and impaired catecholamine-stimulated lipolysis in mice. *J Biol Chem.* 2003;**278**(40):38913-38920.
32. Kitajima K, Nagaya T, Jameson JL. Dominant negative and DNA-binding properties of mutant

thyroid hormone receptors that are defective in homodimerization but not heterodimerization. *Thyroid.* 1995;**5**(5):343-353.

33. Yen PM, Wilcox EC, Hayashi Y, Refetoff S, Chin WW. Studies on the repression of basal transcription (silencing) by artificial and natural human thyroid hormone receptor-beta mutants. *Endocrinology.* 1995;**136**(7):2845-2851.
34. Paquette MA, Atlas E, Wade MG, Yauk CL. Thyroid hormone response element half-site organization and its effect on thyroid hormone mediated transcription. *PLoS One.* 2014;**9**(6):e101155.
35. Chen Y, Young MA. Structure of a thyroid hormone receptor DNA-binding domain homodimer bound to an inverted palindrome DNA response element. *Mol Endocrinol.* 2010;**24**(8):1650-1664.
36. Collingwood TN, Rajanayagam O, Adams M, Wagner R, Cavailles V, Kalkhoven E, Matthews C, Nystrom E, Stenlof K, Lindstedt G, Tisell L, Fletterick RJ, Parker MG, Chatterjee VK. A natural transactivation mutation in the thyroid hormone beta receptor: impaired interaction with putative transcriptional mediators. *Proc Natl Acad Sci U S A.* 1997;**94**(1):248-253.
37. Yoh SM, Chatterjee VK, Privalsky ML. Thyroid hormone resistance syndrome manifests as an aberrant interaction between mutant T3 receptors and transcriptional corepressors. *Mol Endocrinol.* 1997;**11**(4):470-480.
38. Harrus D, Demene H, Vasquez E, Boulahtouf A, Germain P, Figueira AC, Privalsky ML, Bourguet W, le Maire A. Pathological Interactions Between Mutant Thyroid Hormone Receptors and Corepressors and Their Modulation by a Thyroid Hormone Analogue with Therapeutic Potential. *Thyroid.* 2018;**28**(12):1708-1722.

Supplementary Materials

Supplementary Table S1. Primer used for TRα1 mutagenesis.

Mutations	Bases change	Primers (5'-3')
D211G	GAC>GGC	Forward: TGAAGGCTTCCAGGCCCACCTTGTCTCCG Reverse: CGGAGACAAGGTGGGCCTGGAAGCCTTCA
T233A	ACC>GCC	Forward: CGAGTTTACCAAGATCATCGCCCCGGCCATCAC Reverse: GTGATGGCCGGGGCGATGATCTTGGTAAACTCG
M256T	ATG>ACG	Forward: CTGAAGGGGTGCTGCACGGAGATCATGTCCC Reverse: GGGACATGATCTCCGTGCAGCACCCCTTCAG
A263S	GCG>TCG	Forward: GCGGACAGCCGACCGCAGGGACA Reverse: TGTCCCTGCGGTCGGCTGTCCGC
L287V	CTC>GTC	Forward: CAAGCGGGAGCAGGTCAAGAATGGCGG Reverse: CCGCCATTCTTGACCTGCTCCCGCTTG
R384H	CGC>CAC	Forward: CATGTGGAGGAAGTGGCTGGCGTGGCA Reverse: TGCCACGCCAGCCACTTCCTCCACATG
P398H	CCC>CAC	Forward: CACCGAACTCTTCCACCCACTCTTCCTCG Reverse: CGAGGAAGAGTGGGTGGAAGAGTTCGGTG

Supplementary Table S2. Affinity for T3 of TRα1 WT and mutants from the [^{125}I]T3 competitive binding assay.

TRα1	LogKd [Kd (nM)]	LogKd(MT/WT) [Fold Kd]
WT	-0.87±0.10 [0.1]	-
D211G	0.52±0.15 [3.3]	1.39±0.11** [24.5]
T223A	-0.52±0.15 [0.3]	0.35±0.17 [2.2]
M256T	1.34±0.22 [21.9]	2.21±0.15*** [161]
A263S	-0.15±0.24 [0.7]	0.72±0.17* [5.2]
L287V	0.41±0.09 [2.6]	1.28±0.06*** [19.0]
R384H	0.55±0.16 [3.5]	1.41±0.11*** [25.8]
P398H	0.39±0.07 [2.4]	1.25±0.07*** [17.9]
P value$^{\phi}$		<0.001

Data are means ± SEM from four independent experiments (duplicate). *P<0.05, **P<0.01, ***P<0.001 compared with WT=0, One-sample T-test. $^{\phi}$P value of One-way ANOVA compared between mutants.

Supplementary Table S3. T3-dependence of GAL4-NCoR1 dissociation and GAL4-SRC1 association of TRα1 WT and mutants.

TRα1	NCoR1			SRC1		
	$LogIC_{50}$ [IC_{50} (nM)]	$LogIC_{50}$(MT/WT) [Fold IC_{50}]	Max response (%)	$LogEC_{50}$ [EC_{50} (nM)]	$LogEC_{50}$(MT/WT) [Fold EC_{50}]	Max response (%)
WT	-1.09±0.07 [0.1]	-	100	-0.55±0.08 [0.3]	-	100
D211G	-0.02±0.09 [1.0]	1.13±0.07*** [13.6]	98.6±23.9	0.38±0.15 [2.4]	0.95±0.16** [8.9]	103±16.0
T223A	-0.99±0.04 [0.1]	0.15±0.08 [1.4]	84.0±9.2	-0.32±0.11 [0.5]	0.21±0.07 [1.6]	92.2±7.3
M256T	0.78±0.08 [6.0]	1.77±0.10*** [59.5]	77.7±12.3†	1.69±0.08 [48.6]	2.30±0.10*** [200]	79.3±7.3†
A263S	-0.79±0.07 [0.2]	0.37±0.05** [2.3]	89.9±3.6†	-0.19±0.10 [0.7]	0.38±0.11* [2.4]	89.1±9.8
L287V	0.16±0.07 [1.5]	1.30±0.11** [20.1]	115±5.2	0.70±0.08 [5.1]	1.23±0.16** [17.2]	83.4±10.5
R384H	-0.26±0.06 [0.6]	0.90±0.08*** [7.9]	71.7±11.4††	0.36±0.18 [2.3]	0.92±0.18** [8.4]	76.7±14.0
P398H	-0.27±0.11 [0.5]	0.87±0.12** [7.4]	91.7±3.3	0.17±0.10 [1.5]	0.70±0.06** [5.1]	77.3±13.9
*P value*ϕ		<0.001	<0.01		<0.001	NS

Data are means ± SEM from at least four independent experiments (triplicate). *P<0.05, **P<0.01, ***P<0.001 compared with WT=0, and †P<0.05, ††P<0.01, †††P<0.01 compared with WT=100, One-sample T-test. ϕP value of One-way ANOVA compared between mutants (NS=not significant).

Supplementary Table S4. Transcriptional activity of TRα1 WT and mutants tested on three TREs.

TRα1	TREs								
	DR4			IR0			ER6		
	$LogEC_{50}$ [EC_{50} (nM)]	$LogEC_{50}$(MT/WT) [Fold EC_{50}]	Max response (%)	$LogEC_{50}$ [EC_{50} (nM)]	$LogEC_{50}$(MT/WT) [Fold EC_{50}]	Max response (%)	$LogEC_{50}$ [EC_{50} (nM)]	$LogEC_{50}$(MT/WT) [Fold EC_{50}]	Max response (%)
WT	-0.46±0.09 [0.4]	-	100	-0.02±0.16 [1.0]	-	100	-0.40±0.07 [0.4]	-	100
D211G	0.63±0.11 [4.2]	1.06±0.12*** [11.5]	95.3±13.6	1.07±0.13 [11.7]	0.89±0.25* [7.7]	79.6±11.8	1.02±0.16 [10.5]	1.43±0.31* [26.8]	84.5±9.2
T223A	-0.52±0.15 [0.3]	-0.01±0.11 [1.0]	77.6±7.0†	0.10±0.07 [1.3]	-0.07±0.24 [0.8]	73.5±8.7	-0.05±0.17 [0.9]	0.37±0.30 [2.3]	92.6±10.8
M256T	1.57±0.04 [37.5]	2.00±0.12*** [99.7]	108±10.5	1.90±0.16 [78.5]	1.65±0.20* [45.0]	76.9±8.7	1.94±0.26 [87.2]	2.18±0.24* [150]	83.4±9.4
A263S	-0.19±0.06 [0.7]	0.24±0.11 [1.8]	98.2±10.2	0.43±0.16 [2.7]	0.25±0.23 [1.8]	84.9±14.2	0.17±0.08 [1.5]	0.58±0.21 [3.8]	87.4±11.3
L287V	0.91±0.15 [8.1]	1.42±0.22** [26.2]	91.8±9.0	1.58±0.09 [38.3]	1.41±0.26* [25.4]	93.3±6.0	1.64±0.30 [43.7]	2.05±0.43* [111]	94.9±10.6
R384H	0.55±0.09 [3.6]	0.97±0.08** [9.4]	86.3±11.0	0.78±0.07 [6.0]	0.98±0.20* [9.6]	110±13.4	1.04±0.06 [10.9]	1.45±0.14** [28.0]	93.6±2.0†
P398H	0.51±0.16 [3.3]	1.02±0.25* [10.5]	59.2±9.8†	0.87±0.10 [7.4]	0.69±0.20* [4.9]	41.8±6.1†	0.62±0.20 [4.2]	1.03±0.32 [10.7]	83.8±10.2
*P value*ϕ		<0.001	NS		<0.001	<0.01		<0.01	NS

Data are means ± SEM from at least three independent experiments (triplicate). *P<0.05, **P<0.01, ***P<0.001 compared with WT=0, and †P<0.05, ††P<0.01, †††P<0.01 compared with WT=100, One-sample T-test. ϕP value of One-way ANOVA compared between mutants (NS=not significant).

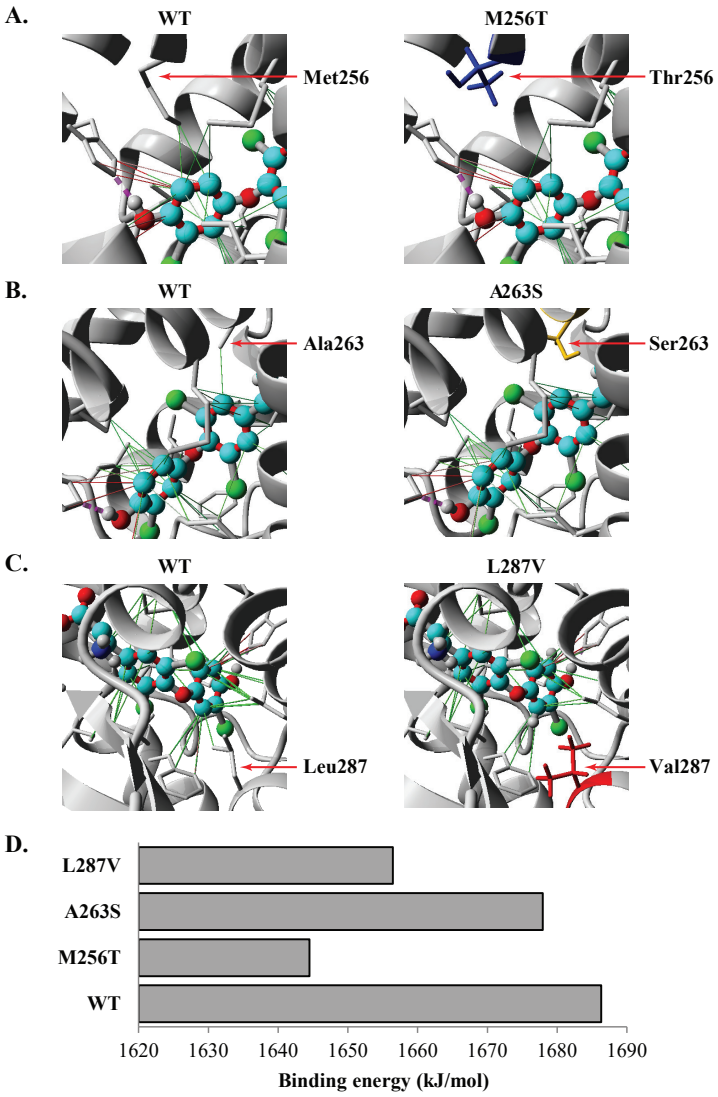

Supplementary Figure S1. (A-C) Close-up views of the wild-type (WT) TRα1 structure (left) and indicated mutant (right) structural models in which the side-chains of all ligand-interacting residues are displayed. The side-chains of the affected residues are indicated with an arrow. WT residues are shown in grey, and mutant residues are highlighted in color. H-bonds are indicated with a purple dashed line, pi-pi interactions with a solid pink line, and hydrophobic interactions with a solid green line. The T3 ligand is displayed in ball-stick style in element colors. All figures were created in YASARA Structure using PovRay imaging software. (D) The bar chart shows reduced T3-binding energy of the mutants predicted by the *in silico* modeling.

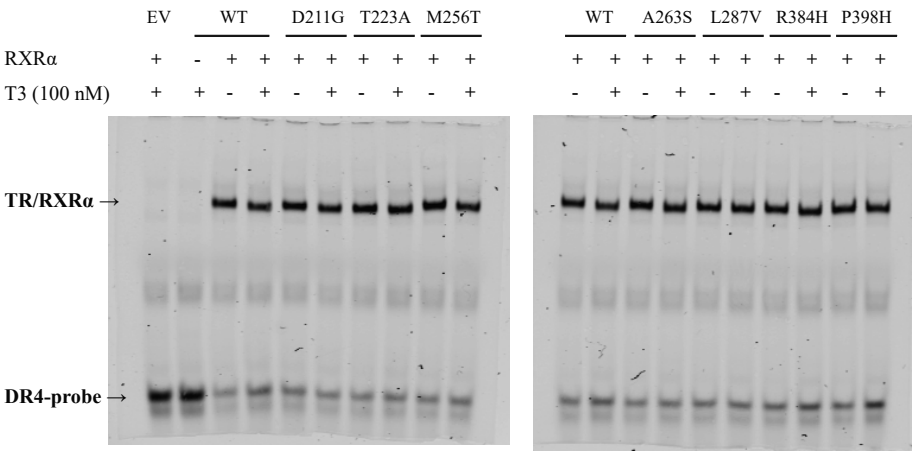

Supplementary Figure S2. Electrophoretic mobility shift assay (EMSA) showing the TR/RXRα heterodimer complex on the DR4-TRE. The heterodimer formation of all mutants is similar to WT and independent of T3 stimulation.

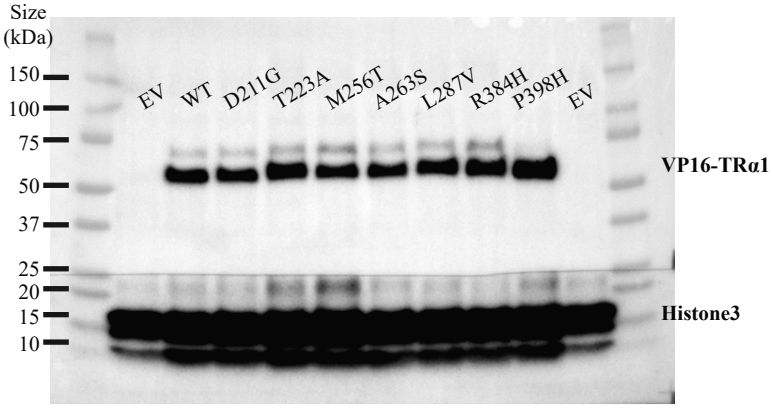

Supplementary Figure S3. Immunoblot confirms the expression of VP16-TRα1 WT and mutants in JEG-3 cells.